Rutaecarpine suppresses atherosclerosis in ApoE$^{-/-}$ mice through upregulating ABCA1 and SR-BI within RCT[S]

Yanni Xu,[1,*] Qi Liu,[1,*] Yang Xu,[*] Chang Liu,[*] Xiao Wang,[*] Xiaobo He,[*] Ningyu Zhu,[*] Jikai Liu,[*] Yexiang Wu,[*] Yongzhen Li,[*] Ni Li,[*] Tingting Feng,[*] Fangfang Lai,[†] Murui Zhang,[§] Bin Hong,[2,*] Jian-Dong Jiang,[2,*,†] and Shuyi Si[2,*]

Institute of Medicinal Biotechnology* and State Key Laboratory of Bioactive Substance and Function of Natural Medicines, Institute of Materia Medica,[†] Chinese Academy of Medical Sciences & Peking Union Medical College, Beijing 100050, China; and Sir Runrun Shaw Hospital of Zhejiang University,[§] Hangzhou, Zhejiang Province 310016, China

Abstract ABCA1 and scavenger receptor class B type I (SR-BI)/CD36 and lysosomal integral membrane protein II analogous 1 (CLA-1) are the key transporter and receptor in reverse cholesterol transport (RCT). Increasing the expression level of ABCA1 and SR-BI/CLA-1 is antiatherogenic. The aim of the study was to find novel antiatherosclerotic agents upregulating expression of ABCA1 and SR-BI/CLA-1 from natural compounds. Using the ABCA1p-LUC and CLA-1p-LUC HepG2 cell lines, we found that rutaecarpine (RUT) triggered promoters of ABCA1 and CLA-1 genes. RUT increased ABCA1 and SR-BI/CLA-1 expression in vitro related to liver X receptor alpha and liver X receptor beta. RUT induced cholesterol efflux in RAW264.7 cells. ApoE-deficient (ApoE$^{-/-}$) mice treated with RUT for 8 weeks showed ~68.43, 70.23, and 85.56% less en face lesions for RUT (L), RUT (M), and RUT (H) groups, respectively, compared with the model group. Mouse macrophage-specific antibody and filipin staining indicated that RUT attenuated macrophages and cholesterol accumulations in atherosclerotic lesions, respectively. Additionally, ABCA1 and SR-BI expression was highly induced by RUT in livers of ApoE$^{-/-}$ mice. Meanwhile, RUT treatment significantly increased the fecal ^{3}H-cholesterol excretion, which demonstrated that RUT could promote RCT in vivo. RUT was identified to be a candidate that protected ApoE$^{-/-}$ mice from developing atherosclerosis through preferentially promoting activities of ABCA1 and SR-BI within RCT.—Xu, Y., Q. Liu, Y. Xu, C. Liu, X. Wang, X. He, N. Zhu, J. Liu, Y. Wu, Y. Li, N. Li, T. Feng, F. Lai, M. Zhang, B. Hong, J-D. Jiang, and S. Si. **Rutaecarpine suppresses atherosclerosis in ApoE$^{-/-}$ mice through upregulating ABCA1 and SR-BI within RCT. *J. Lipid Res.* 2014.** 55: **1634–1647.**

Supplementary key words apolipoprotein E deficient • ATP binding cassette transporter A1 • scavenger receptor class B type I • reverse cholesterol transport

Excessive accumulation of cholesterol in macrophages results in a transformation of the macrophage into foam cells and eventually causes atherosclerosis (1, 2). The pathogenic process represents a chronic and complicated interaction involving multiple factors. Reverse cholesterol transport (RCT) is a process by which extrahepatic (peripheral) cholesterol is returned to the liver for excretion in the bile and ultimately the feces, thus reducing the risk of atherosclerosis (3, 4). Although there have been great efforts in discovering drugs against atherosclerosis (5), the output has been unsatisfactory. Removal of excess cholesterol from macrophage foam cells is considered to be one of the therapeutic strategies (6). The crucial cellular transporters and receptors that relate to cholesterol efflux include,

Abbreviations: Ac-LDL, acetylated LDL; ALT, alanine transaminase; ApoE$^{-/-}$, ApoE deficient; AST, aspartate aminotransferase; CBP, CREB-binding protein; CLA-1, CD36 and lysosomal integral membrane protein II analogous 1; CMC-Na, carboxymethylcellulose sodium; DiI-HDL, 1,1′-dioctadecyl-3,3,3′,3′-tetramethylindocarbocyanine perchlorate-labeled HDL; DRIP, vitamin D receptor interacting protein; GAL-4, yeast transcription activator; H&E, hematoxylin and eosin; HDL-C, HDL cholesterol; HFD, high-fat diet; ID, interaction domain; LBD, ligand binding domain; LDL-C, LDL cholesterol; LXRα, liver X receptor alpha; LXRβ, liver X receptor beta; MAC-3, mouse macrophage-specific antibody; NCoR, nuclear corepressor; NR, nuclear receptor; ORO, Oil Red O; Ox-LDL, oxidized LDL; PGC, PPAR-γ coactivator; RCT, reverse cholesterol transport; RUT, rutaecarpine; SMRT, silencing mediator for retinoid and thyroid hormone receptors; SR-BI, scavenger receptor class B type I; SRC, steroid receptor coactivator; SREBP-1c, sterol-regulatory element binding protein 1c; TC, total cholesterol; TR-FRET, time-resolved fluorescence resonance energy transfer.

[1] Y. Xu and Q. Liu contributed equally to this article.

[2] To whom correspondence should be addressed.
e-mail: sisyimb@hotmail.com (S.S.); jiang.jdong@163.com (J-D. J.); binhong69@hotmail.com (B.H.)

[S] The online version of this article (available at http://www.jlr.org) contains supplementary data in the form of three figures and two tables.

This work was supported by grants from the Key New Drug Creation and Manufacturing Program (2012ZX09301002-003 and 2012ZX09301002-001); the National Natural Science Foundation of China (81102443, 81273515, 81321004, and 90813027); PUMC Youth Fund (3332013089), the Fundamental Research Funds for the Central Universities (3332013089); and the National Natural Science Foundation of China-Guangdong Provincial People's Government of the Joint Natural Science Fund Projects (U1032007). Conflict of interest: none declared.

Manuscript received 18 September 2013 and in revised form 6 June 2014.

Published, JLR Papers in Press, June 7, 2014
DOI 10.1194/jlr.M044198

at least, ABCA1 and scavenger receptor class B type I (SR-BI) (3, 7, 8).

ABCA1 is one of the ABC superfamily members. It promotes cholesterol and phospholipid efflux from cells to lipid-poor ApoA-I and facilitates RCT. Loss-of-function mutations in the ABCA1 gene result in Tangier disease, showing plasma deficiency of HDL and increase susceptibility to atherosclerosis (8–11). Transgenic mice that expressed a high level of ABCA1 had increased cholesterol efflux in macrophages and exhibited a low incidence of developing atherosclerosis (12, 13). Selective inactivation of macrophage ABCA1 in mice resulted in a substantial increase of atherosclerosis (12, 13). Therefore, upregulation of ABCA1 gene expression becomes an attractive strategy against atherosclerosis (10, 14).

SR-BI is a specific receptor for HDL. Human homolog of the murine SR-BI gene, hSR-BI, is called CLA-1 (CD36 and lysosomal integral membrane protein II analogous 1) (15). SR-BI could facilitate hepatic uptake of HDL cholesterol (HDL-C) of the RCT pathway, as well as HDL-mediated cholesterol efflux from the arterial wall (16, 17). CHO cells transfected with SR-BI had their cholesterol efflux largely increased (18). Experiments using transgenic and gene knockout mice have demonstrated the antiatherogenic effect of SR-BI (19). Thus, increasing SR-BI expression and/or activity in the liver or the artery wall is thought to be desirable as an antiatherogenic therapeutic approach (17).

The goal of this study was to identify small-molecular upregulators of ABCA1 and SR-BI/CLA-1 expression from 20,000 natural or synthetic compounds using the high-throughput screening models that we have established (20, 21). After several rounds of screening, we found for the first time that the natural compound rutaecarpine (RUT) upregulated expression of the two target genes (ABCA1 and SR-BI/CLA-1) at the same time without cytotoxicity on the screening cells. In what is described subsequently, we show the upregulatory activity of RUT on ABCA1 and SR-BI/CLA-1 and the antiatherosclerotic therapeutic potential of the compound in ApoE-deficient ($ApoE^{-/-}$) mice.

METHODS

Cell cultures

Human hepatoma HepG2 cells, ABCA1p-LUC HepG2 (20), CLA1p-LUC HepG2 (21), and murine peritoneal macrophage cell line RAW264.7 (22) were maintained by our laboratory. HepG2 cells were grown in MEM medium (Hyclone) supplemented with 10% heat-inactivated FBS (medium A). RAW264.7 cells were passaged in DMEM (Hyclone) containing 10% FBS (medium B). J774 cells were obtained from (Institute of Basic Medical Sciences, Chinese Academy of Medical Sciences and Peking Union Medical College, China) and grown in RPMI 1640 (Hyclone) supplemented with 10% FBS (medium C). A stable transformed ABCA1p-LUC HepG2 cell line was maintained in medium C supplemented with 10% FBS and 500 μg/ml G418 (medium D). A stable transformed CLA1p-LUC HepG2 cell line was maintained in medium E (medium B supplemented with 600 μg/ml G418).

Chemicals

RUT was obtained from Shaanxi Sciphar Hi-tech Industry Co. Ltd. (Xi'an, China). The 9-*cis*-retinoic acid , BSA, T0901317, and G418 were obtained from Sigma. Simvastatin was from the National Institute for Food and Drug Control (Beijing, China). Human ApoA-I, acetylated LDL (Ac-LDL), and oxidized LDL (Ox-LDL) were purchased from Peking Union-Biology Co. Ltd (Beijing, China). The 1,1′-dioctadecyl-3,3,3′,3′-tetramethylindocarbocyanine perchlorate (DiI)-labeled HDL (DiI-HDL) was from Biomedical Technologies Inc. (MA).

$ApoE^{-/-}$ mice for atherosclerosis analysis

Animals used for experiments were 8-week-old female C57/BL6 $ApoE^{-/-}$ mice weighing 18–20 g (Peking University Animal Center). The mice were randomly divided into six groups of 12 mice each. The mice on the chow diet received carboxymethylcellulose sodium (CMC-Na) as the untreated control group. Mice on the high-fat diet (HFD) (0.15% cholesterol and 20% fat) received CMC-Na as the model group, simvastatin (5 mg/kg), or RUT [10, 20, and 40 mg/kg, as RUT (L), RUT (M) and RUT (H), respectively]. RUT and simvastatin were given intragastrically daily. Body weight and survival were monitored.

After 8 weeks of HFD feeding, mice were fasted for 6 h, and blood samples were taken from the retro-orbital plexus, before mice were euthanized for analysis. Total cholesterol (TC), HDL-C, LDL cholesterol (LDL-C), and TG levels were measured using commercially available kits (Biosino Bio-technology and Science Inc., China) (23). The liver and intestine were harvested, snap-frozen in liquid nitrogen, and stored at −80°C for cholesterol, RT-PCR, and Western blot analysis. The aorta, heart, and liver were placed in 4% formalin for 6 h at 37°C and then stored at 20% sucrose for atherosclerotic lesion analysis (24). For 24 h, feces were collected from cages of each group during the last day of the treatment (25). Mice were kept in their original cages to avoid stressful procedures. Feces were freeze-dried, weighed, and ground before storage at −20°C. The TC content in liver, intestine, or feces was measured by using a tissue cholesterol assay kit (Applygen Technologies Inc., China) by a microplate reader (EnVision, PerkinElmer). The lysis buffer was added 20 μl/mg liver and 10 μl/mg intestine or feces. Proteins were measured using BCA assay kit (Pierce). Cholesterol content was expressed as micromoles TC per gram protein (26).

Animal care and experimental procedures were performed in accordance with the regulations of the Institutional Animal Care and Use Committee of the Institute of Medicinal Biotechnology Institute.

Analysis of atherosclerosis in atherosclerotic mice

$ApoE^{-/-}$ mice were euthanized and perfused with 20 ml 0.01 M PBS through the left ventricle. Aortas were dissected from the proximal ascending aorta to the bifurcation of the iliac artery, and adventitial fat was removed (24). The aorta and heart were fixed in 4% formalin for 6 h at 37°C, and then stored in 20% sucrose. The heart with ascending aorta was then embedded in OCT, snap-frozen in liquid nitrogen, and stored at −80°C prior to sectioning on a Leica cryostat. For analyzing aortic sinus plaque lesions, serial 7 μm cryosections were obtained working from the apex of the heart toward the origin of the aorta. For en face analysis, aortas were split longitudinally (27). Sections and fixed aortas were stained with Oil Red O (ORO) for 30 min and rinsed (28). Images of the ORO staining sections and the open luminal surface of the vessels were captured with a Leica Q550cw Graphic Analysis System and a digital camera (Sony), respectively. Total aortic areas and atherosclerotic lesion areas were measured and quantified using an ImageJ Graphic Analysis System (29).

Histology and immunohistochemical staining

Hematoxylin and eosin (H&E) staining was performed from livers on paraffin sections (5 μm) for morphometric analysis. All sections were examined under a Nikon E600 microscope. Mouse macrophage-specific antibody (Mac-3) immunochemistry staining and Filipin staining were performed on the cryosections (7 μm) from aortic sinus using Mac-3 monoclonal antibody (BD Pharmingen™) and a Filipin staining kit (Genmed Sci), respectively. Mac-3 staining slides were examined with a light microscope at 200× magnification (24). The Filipin staining images were viewed under a fluorescence microscope (excitation 340 nm, emission 430 nm) at 200× magnification. Both positive and negative control slides were processed at the same time in each experiment.

Macrophage in vivo RCT studies in C57/BL6 and C57/BL6 ApoE$^{-/-}$ mice

Macrophage in vivo RCT studies were performed as described by Zhang et al. (30–32). In brief, 12 6- to 8-week-old male C57/BL6 mice were treated with RUT (20 mg/kg/day) or CMC-Na for 14 days. Twelve 6- to 8-week-old male ApoE$^{-/-}$ mice on HFD were treated with RUT (20 mg/kg) or CMC-Na for 8 weeks. The treatment was continued during the 48 h RCT study.

J774 cells were grown in medium C and radiolabeled with 5 μCi/ml ^{3}H-cholesterol (PerkinElmer, Waltham, MA) and cholesterol enriched with 100 μg/ml of Ac-LDL for 48 h. These foam cells were washed twice, equilibrated in medium with 0.2% BSA for 6 h, spun down, and resuspended in 1640 medium.

On the day of injection, animals were caged individually with unlimited access to food and water. ^{3}H-cholesterol-labeled J774 foam cells (about 3×10^6 cells containing 2×10^6 cpm in 0.5 ml 1640 medium) were injected intraperitoneally. Animals continued to receive CMC-Na or RUT during the 48 h RCT study. At 48 h, mice were anesthetized and perfused with cold PBS. Livers were removed and stored at −20°C until lipid extraction. Blood was collected at 48 h, and plasma was used for liquid scintillation counting (LSC) and lipoprotein analysis. Feces were collected continuously from 0 to 48 h and were stored at 4°C until extraction of cholesterol and bile acid.

Liver, fecal, and bile cholesterol analyses

Liver lipids, fecal cholesterol, and bile acid were extracted as described by Zhang et al. (30–34). Briefly, a 100 mg piece of liver tissue was homogenized in water and extracted three times with 9 ml chloroform-methanol (2:1, v/v). The extracts were pooled, evaporated, resuspended in toluene, and then counted in a liquid scintillation counter. The total feces collected from 0 to 48 h were weighed and soaked in Millipore water (1 ml water/100 mg feces) overnight at 4°C. The next day, an equal volume of ethanol was added, and the samples were homogenized. A 200 μl aliquot of each homogenized fecal sample was counted in a liquid scintillation counter to establish the ^{3}H-total sterols. To extract the ^{3}H-cholesterol and ^{3}H-bile acid fractions, 2 ml of the homogenized samples was combined with 2 ml ethanol and 400 μl 1 M NaOH. The samples were saponified at 95°C for 2 h and cooled to room temperature, and then ^{3}H-cholesterol was extracted three times with 9 ml hexane. The extracts were pooled, evaporated, resuspended in toluene, and then counted in a liquid scintillation counter. To extract ^{3}H-bile acids, the remaining aqueous portion of the feces was acidified with concentrated HCl and then extracted three times with 9 ml hexane. The extracts were pooled together, evaporated, resuspended in toluene, and counted in a liquid scintillation counter.

Luciferase reporter assay and transient transfection

GAL-4 is a yeast transcription activator. The GAL4 chimeric receptor expression vectors [pBIND-LXRα-LBD (ligand binding domain, LBD) and pBIND-LXRβ-LBD] were constructed as previously described (35). ABCA1, CLA-1 transcriptional activity assay, and pBIND-LXRα/LXRβ-LBD/GAL4 chimera reporter assay were performed as previously described using ABCA1p-LUC HepG2 (20), CLA1p-LUC HepG2 (21), and HepG2 cells, respectively. And these cells were treated with RUT at the indicated concentrations for 18 h at 37°C. The luciferase activity was measured using the Luciferase Assay System (Promega).

Cholesterol efflux assay

RAW264.7 cells were plated into 24-well plates (Costar) and labeled with 0.5 ml of labeling medium, serum-free DMEM supplemented with 0.2% (w/v) BSA (Sigma Chemical) (medium F) and containing 1 μCi/ml ^{3}H-cholesterol. After 24 h of labeling, cells were washed twice and equilibrated for 24 h with or without RUT in 0.5 ml medium F. At the end of the treatment period, cells were washed twice with PBS and incubated with 0.5 ml of medium F, with or without 10 μg/ml ApoA-I or 50 μg/ml HDL as the final concentration at 37°C. After incubation for 4 h, the medium was collected and clarified by centrifugation in a microcentrifuge for 2 min. Cells were lysed using 500 μl of 0.1 M NaOH for 30 min. The radioactivities of supernatant and cell lysates were determined by LSC. The percentage of ^{3}H-cholesterol efflux was calculated as 100 × (medium cpm)/(medium cpm + cell cpm). The ratio of ^{3}H-cholesterol efflux was calculated as the percentage cholesterol efflux of each sample/control (36, 37).

Foam cell assay

RAW 264.7 cells were plated in 96-well or 6-well plates (Costar) at 5×10^5 cells/ml. After 6 h, the cells were refed with Ac-LDL or Ox-LDL (80 μg/ml) in DMEM for 24 h. Then cultures were removed, and cells were washed with PBS. RUT (0.035, 0.35, 3.48, and 34.80 μM) was added for a further 24 h. At the end, the cells were stained with ORO or handled with cell lysis buffer for quantitative assay. The ORO staining procedures were the same as previously described (17). The contents of TC and free cholesterol were measured using a cholesterol/cholesteryl ester quantitation colorimetric kit (BioVision) and expressed as μg per 10^6 cells every well.

Cellular uptake of DiI-HDL

Cellular uptake DiI-HDL assay was performed as described by Liu et al. (38). HepG2 cells were incubated with RUT (0.035, 0.35, 3.48, and 34.80 μM) in MEM medium for 24 h. After incubation, the cells were washed twice with PBS and incubated with DiI-HDL (5 μg/ml) at 37°C for additional 4 h. At the end of incubation period, cells were washed and examined by Eclipse TE2000-U Inverted Microscope (Nikon,Tokyo, Japan). The DiI-HDL uptake was determined by a microplate reader (EnVision) and expressed as fold of the control (DiI-HDL).

Quantitative real-time RT-PCR

Total RNA from cells or tissues was extracted using TRIzol (Invitrogen) and reverse transcribed (Fermentas). PCR amplification was then performed using FastStart Universal SYBR Green Master (Roche) with specific primers (**Table 1**). The relative signal intensity was measured using an iQ5 Multicolor Real-Time PCR Detection System (Bio-Rad). All of values were normalized against that of β-actin (39).

Western blots

Aliquots (50 μg) of cell lysates or liver proteins from different subgroups of ApoE$^{-/-}$ mice were separated on 10% SDS-PAGE as described previously (40, 41). The primary antibodies used for the Western blot were the following: ABCA1 (1:500, NB400-105, Novus Biologicals); SR-BI (1:1000, NB400-104, Novus Biologicals);

TABLE 1. Sequences of primers for real-time quantitative PCR

Genes	Forward Primer (5′ to 3′)	Reverse Primer (5′ to 3′)
h-ABCA1	GCCTGCTAGTGGTCATCCTG	CCACGCTGGGATCACTGTA
h-CLA-1	TTCTGCCCGTGCCTGGAGTC	GCTGTCTGCTGGGAGAGTC
h-CD36	CCTCCTTGGCCTGATAGAAA	GTTTGTGCTTGAGCCAGGTT
h-SREBP-1c	CGGAGCCATGGATTGCACTTTC	GATGCTCAGTGGCACTGACTCTTC
h-FAS	AAGGACCTGTCTAGGTTTGATGC	TGGCTTCATAGGTGACTTCCA
h-β-actin	CCAACCGCGAGAAGATGA	CCAGAGGCGTACAGGGATAG
m-ABCA1	GGGTCTGAACTGCCCTACCT	TACTCCCCTGATGCCACTTC
m-SR-BI	GCCCATCATCTGCCAACT	TCCTGGGAGCCCTTTTTACT
m-CD36	TTGTACCTATACTGTGGCTAAATGAGA	CTTGTGTTTTGAACATTTCTGCTT
m-ABCG1	AGGTCTCAGCCTTCTAAAGTTCCTC	TCTCTCGAAGTGAATGAAATTTATCG
m-SREBP-1c	CCGAGCATTCCAACTGGTG	CCATGTTCGGGAAGTAGGCT
m-FAS	GGAGGTGGTGATAGCCGGTAT	TGGGTAATCCATAGAGCCCAG
m-β-actin	CTAAGGCCAACCGTGAAAG	ACCAGAGGCATACAGGGACA

h, human; m, mouse; SREBP-1c, sterol-regulatory element binding protein 1c.

CD36 (H300, 1:500, Santa Cruz); ABCG1 (1945-1, 1:500, EPIT MICS); liver X receptor alpha (LXRα; ab41902, 1:500, Abcam); liver X receptor beta (LXRβ; sc-1001, 1:400, Santa Cruz); SREBP-1c (ab135133, 1:500, Abcam); FAS (F9554, 1:1000, Sigma); GAPDH (sc-25778, 1:1000, Santa Cruz;); and β-actin (A5441, 1:5000, Sigma).

siRNA against LXRα and LXRβ

siRNA against human LXRα (siG11610160927, forward sequence 5′-GGAUGCUAAUGAAACUGGU dTdT-3′, reverse sequence 3′-dTdT CCUACGAUUACUUUGACCA-5′, Guangzhou RiboBio Co. Ltd., China), LXRβ (sc-45316, Santa Cruz), and scrambled siRNA for the negative control (sc-37007, Santa Cruz) were used. Briefly, HepG2 cells were plated in 6-well plates (Costar). After 6 h, the cells were transfected with or without scrambled siRNA (50 nM), LXRα siRNA (50 nM), or LXRβ siRNA (50 nM) using RNAi MAX transfection reagent (Roche) for 48 h. Then the cultures were removed, and cells were incubated with or without RUT (0.35 and 3.48 μM) for a further 24 h. Compared with the control siRNA, the LXRα siRNA (50 nM) and LXRβ siRNA (50 nM) suppressed the expression of LXRα and LXRβ mRNA by 90% and 75%, respectively, according to the real-time quantitative PCR assays (data not shown). ABCA1 and SR-BI protein levels were determined by Western blotting assays.

TR-FRET LXRα/β coregulator peptide interaction assay

Time-resolved fluorescence resonance energy transfer (TR-FRET) LXRα/β coregulator peptide interaction assays were performed using the LanthaScreen™ TR-FRET Liver X Receptor α (PV4655) or β (PV4658) Coactivator Assay Kit (Invitrogen, Carlsbad, CA) according to the manufacturer's instructions. Human coregulator peptides were synthesized and conjugated to fluorescein by Invitrogen: Fluorescein-thyroid hormone receptor associated protein (TRAP)220/vitamin D receptor interacting protein (DRIP)-250 (PV4604), Fluorescein-TRAP220/DRIP-2 (PV4549), Fluorescein-D22 (PV4386), Fluorescein-SRC1-2 (PV4578), Fluorescein-steroid receptor coactivator (SRC)1-4 (PV4582), Fluorescein-SRC2-2 (PV4586), Fluorescein-SRC3-3 (PV4594), Fluorescein-PPAR-γ coactivator (PGC)1α (PV4421), Fluorescein-CREB-binding protein (CBP)-1 (PV4596), Fluorescein-nuclear receptor co-repressor (NCoR) interaction domain (ID)2 (NCoR 2, PV4624), and Fluorescein-silencing mediator of retinoic and thyroid hormone receptors (SMRT) ID2 (PV4423). T0901317 or RUT was diluted and first added to 384-well black plates (Costar) according to the kits' instructions. LXRα/β LBD was then added, and a mixture of coregulator and LanthaScreen™ Tb-anti-GST antibody was added last. The plates were covered, shaken briefly, and incubated at room temperature for 4 h. The data were calculated as the ratio of the emission intensity of the acceptor (fluorescein: 520 nm) divided by the emission intensity of the donor (Tb: 490 nm). Experiments were repeated twice.

Statistics

The results are expressed as means ± SEM of at least three independent experiments. Statistical analysis was performed using the Student's *t*-test. A two-sided *P* value of <0.05 was considered to indicate statistical significance.

RESULTS

RUT upregulated ABCA1 and CLA-1/SR-BI expression in vitro

A total of 20,000 compounds, at a final concentration of 10 μg/ml, were screened for ABCA1 and CLA-1 upregulator candidates. The compounds were from the compound library of the Institute of Medicinal Biotechnology, Chinese Academy of Medical Sciences. Hit compounds that were selected should upregulate expression of, at least, both ABCA1 and CLA-1.

Among the 20,000 compounds, RUT (**Fig. 1A**) tested positive in stimulating promoters of both ABCA1 and CLA-1 genes and therefore upregulating their expression. RUT induced ABCA1 transcription in the ABCA1p-LUC HepG2 cells, with an EC_{50} of 0.27 μM and a maximal value of 240% (Fig. 1B); it also stimulated CLA-1 transcription in the CLA1p-LUC HepG2 cells, with an EC_{50} of 0.15 μM and a maximal value of 170% (Fig. 1C). This activity was dose dependent in both ABCA1 and CLA-1.

To confirm the upregulatory activity of RUT in the luciferase reporter assay, RUT's effect on ABCA1 and CLA-1/SR-BI mRNA and protein expression was examined in HepG2 and RAW264.7 cells, respectively. RT-PCR assay in HepG2 and RAW264.7 cells showed that the mRNA levels of ABCA1 and CLA-1/SR-BI were significantly upregulated by RUT (0.35 μM) (Fig. 1D, F). Western blot analysis in HepG2 cells showed that ABCA1 and CLA-1 protein levels increased when incubated with 0.035, 0.35, 3.48, or 34.80 μM of RUT,

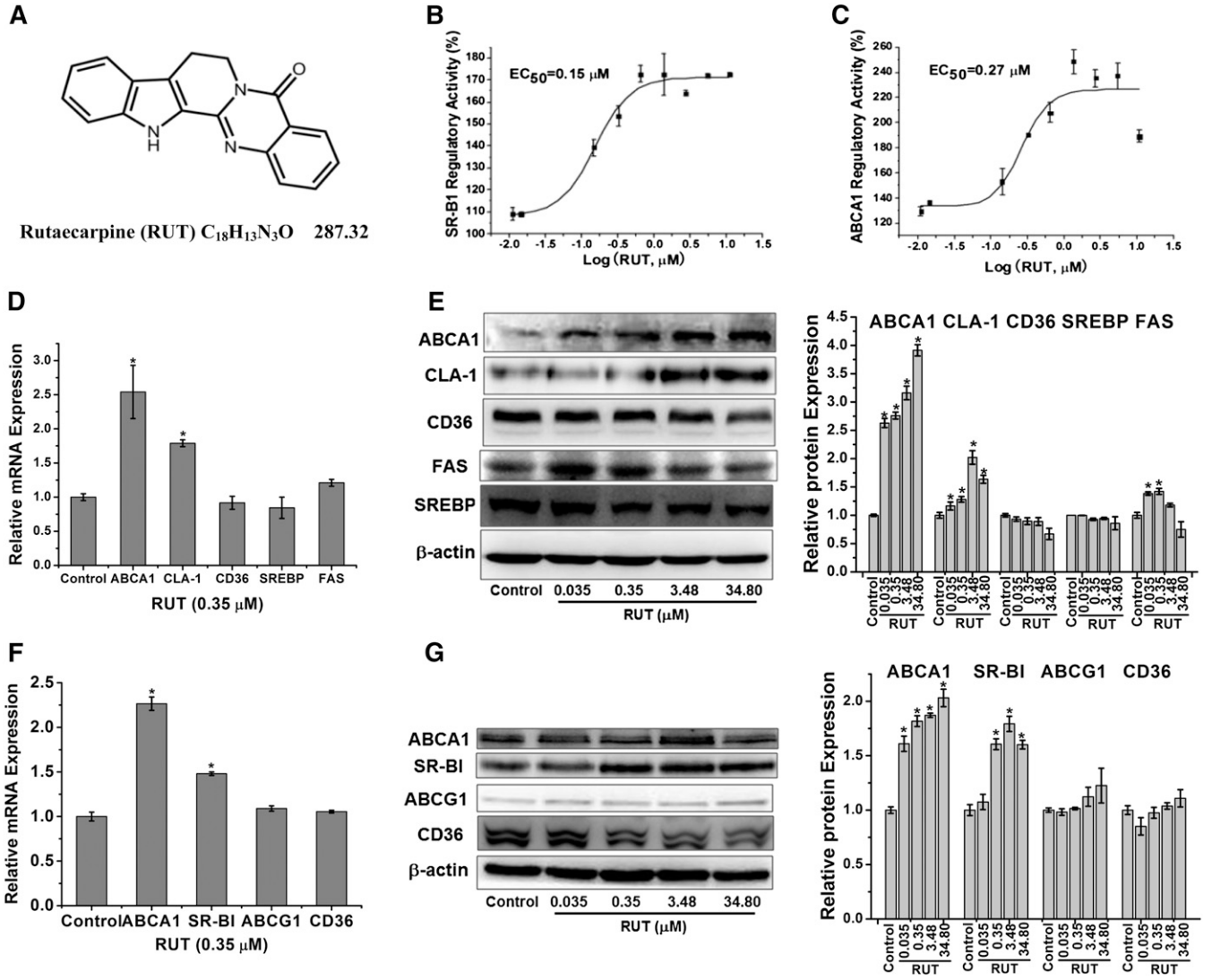

Fig. 1. The multiple target nature of RUT in vitro. Chemical structure of RUT (A); dose-dependent curves for RUT (in log scale) in ABCA1p-LUC HepG2 cells (B) and CLA-1p-LUC HepG2 cells (C). Quantitative data are the mean ± SEM from at least three separate experiments; mRNA levels in HepG2 cells (D) and RAW264.7 cells (F) of indicated genes were determined by real-time PCR, respectively. Data are expressed as means ± SEM of three independent experiments and are relative to that of control. * $P < 0.05$ versus control. Protein levels in HepG2 cells (E) and RAW264.7 cells (G) of indicated genes were determined by Western blotting, respectively. A representative immunoblot in HepG2 cells (E) and RAW264.7 cells (G) is shown, respectively, and the abundances were normalized to that of β-actin. Data are expressed as means ± SEM of three independent experiments and are relative to that of control. * $P < 0.05$ versus control.

with a maximum increase of 3.91- and 2.02-fold for these two proteins, respectively (Fig. 1E). Western blot analysis in RAW264.7 showed that ABCA1 and CLA-1 protein levels increased when incubated with RUT, with a maximum increase of 2.06- and 1.78-fold for these two proteins, respectively (Fig. 1G). In addition, ABCA1 and SR-BI protein expression levels treated with RUT were also significantly upregulated in primary murine macrophages from female Institute of Cancer Research (ICR) mice (data not shown), in accordance with the result in RAW264.7 cells.

Recent studies indicated that ABCG1 could promote cholesterol efflux. SREBP-1c is a transcription factor known to regulate the expression of the lipogenic gene. FAS plays an important role in diet-induced atherosclerosis. CD36, a member of the SR-B family, plays a significant role in macrophage binding and uptake of Ox-LDL. Therefore, the effect of RUT on SREBP-1c, FAS, ABCG1, and CD36 was then examined. Data showed that the protein expression of SREBP-1c in HepG2 (Fig. 1E), and CD36 (Fig. 1G) in RAW264.7, was not upregulated by RUT. The ABCG1 protein level in RAW264.7 was slightly upregulated by RUT at 34.80 μM (Fig. 1G). The FAS protein level was modestly upregulated by RUT at 0.035 and 0.35 μM (Fig. 1 E). Our data suggest a preference of RUT for the key components ABCA1 and SR-BI within the RCT network.

RUT regulated ABCA1 and CLA-1/SR-BI expression by LXRα and LXRβ

The pBIND-LXRα/LXRβ-LBD/GAL4 chimera reporter assay showed that RUT could activate LXRα/LXRβ-LBD, with an EC_{50} of 0.0030 and 0.0014 μM (**Fig. 2A**, **B**), respectively.

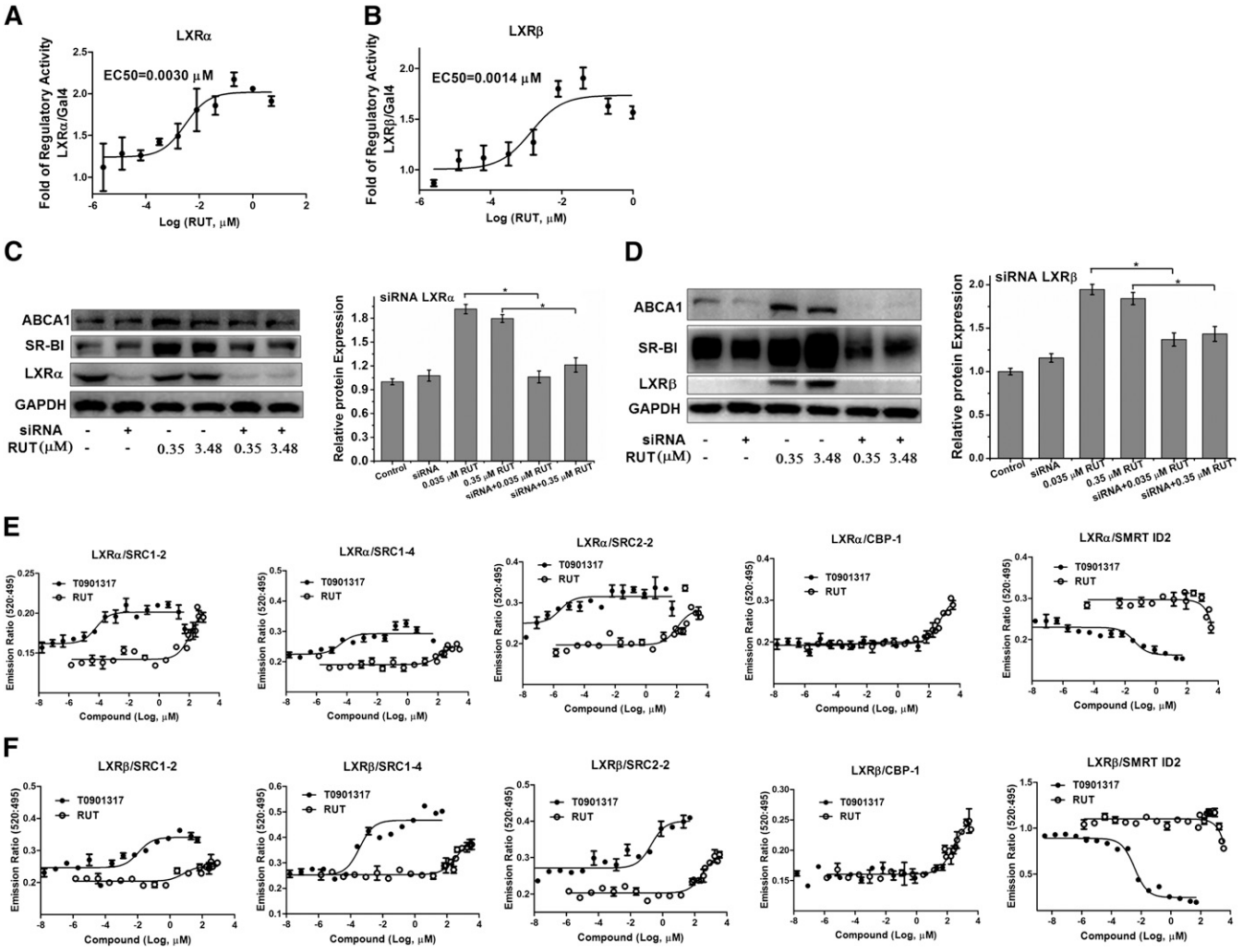

Fig. 2. Regulation of RUT on ABCA1 and SR-BI expression by LXRα and LXRβ. A, B: GAL4 chimeric receptor assay. pBIND-LXRα-LBD (A) or pBIND-LXRβ-LBD (B) was cotransfected with GAL4 reporter vector into HepG2 cells. Experiments were carried out in triplicate wells and repeated at least thrice. Results are expressed in terms of fold induction over control (0.1% DMSO). C, D: HepG2 cells were incubated with or without RUT (0.035, 0.35, 3.48, and 34.80 μM), scrambled siRNA (50 nM), LXRα siRNA (50 nM) (C), or LXRβ siRNA (50 nM) (D) for 18 h, and then the levels of ABCA1 and SR-BI proteins were determined by Western blotting assays. A representative immunoblot of three separate experiments is shown, and the abundances of indicated proteins were normalized to that of GAPDH when treated LXRα siRNA (C) and LXRβ siRNA (D). Data are means ± SEM (* $P < 0.05$). E, F: TR-FRET assay was used to examine corepressor peptide displacement from or coactivator recruitment to human LXRα (E) or LXRβ (F) LBD in response to T0901317 or RUT. The data were calculated as the ratio of 520 nm/495 nm. Figures are representative of at least two independent experiments.

To examine whether the regulatory function of RUT on ABCA1 and SR-BI/CLA-1 was related with LXRα or LXRβ activity, siRNA knock-down experiments on LXRα or LXRβ in HepG2 cells were performed, respectively. HepG2 cells were treated as described in Methods. Western blotting analysis showed that the upregulating effects of RUT on ABCA1 and SR-BI markedly decreased when LXRα (Fig. 2C) or LXRβ was silenced (Fig. 2D), which indicated that RUT regulated ABCA1 and SR-BI expression through the LXRα and LXRβ pathway.

Ligand-dependent nuclear receptor (NR) activation regulates target gene expression through interactions with a variety of transcriptional coactivator and corepressor proteins. To monitor the unique receptor conformation induced upon RUT binding and transcriptional regulatory proteins, we compared the ability of RUT and T0901317 to modulate the interaction of corepressors and coactivators with LXRα or LXRβ LBD using a TR-FRET assay. As shown in Fig. 2E, F, distinct patterns of coregulator recruitment to LXRα/LXRβ were observed in response to RUT and T0901317. Coactivator peptides including SRC1-2, SRC1-4, and SRC2-2 recruitment by RUT were similar to the degree of T0901317. Slightly better recruitment by RUT was seen for CBP-1 than T0901317. Corepressor peptide SMRT ID2 was partially displaced from both LXRα and LXRβ LBDs by RUT compared with T0901317. Coactivator peptides exhibited partial recruitment to both LXRα and LXRβ LBDs by RUT compared with T0901317, including TRAP220/DRIP-2, D22, TRAP220/DRIP-250, PGC1α,

and SRC3-3 (supplementary Fig. II). Corepressor peptide NCoR ID2 was partially displaced from LXRβ LBD but not LXRα LBD by RUT compared with T0901317 (supplementary Fig. II). These results suggest that RUT can induce a distinct receptor conformation upon binding LXRα and LXRβ LBDs that could result in a unique pattern of coactivator and corepressor protein recruitment.

RUT promoted cholesterol efflux and inhibited lipid accumulation in vitro

Based on the fact that RUT regulates the expression of ABCA1 and SR-BI/CLA-1, we surmised that RUT might play roles in modulating cholesterol efflux from macrophage cells and increasing HDL uptake in HepG2 cells. RUT at a final concentration of 0.035, 0.35, 3.48, or 34.80 μM was used in these assays, and DMSO (0.1%) was used as a negative control.

As shown in **Fig. 3A**, **B**, treatment of RAW264.7 cells with RUT resulted in a significant increase of cholesterol efflux to extracellular ApoA-I (Fig. 3A) or HDL (Fig. 3B) with a maximal activity of 2- and 2.5-fold, respectively. Treating RAW 264.7 with Ac-LDL (Fig. 3C) or Ox-LDL (80 μg/ml) (Fig. 3D) induced foam cell formation, which was characterized with increased lipid storage in cytoplasm. Here, we showed that RUT significantly ameliorated intracellular lipid accumulation as determined by ORO staining (Fig. 3C, D) and by the measurement of cellular cholesterol content (Fig. 3E, F). It should be noted that Ox-LDL (80 μg/ml) led to some cell damage and increased about 13.71 ± 0.50% in early apoptosis compared with control (about 2.88 ± 0.18%) (data not shown). We next examined the effect of RUT on HDL uptake in HepG2 cells. We found that RUT significantly increased DiI-HDL uptake in HepG2 cells (Fig. 3G, H) through SR-BI/CLA-1. In addition, RUT inhibited Ac-LDL-induced foam cell formation in primary murine macrophages from female ICR mice (data not shown), which is in accordance with the result in RAW264.7 cells.

Taken together, these data suggest that RUT protects against the formation of macrophage foam cells by increasing ABCA1- and SR-BI/CLA-1-mediated cholesterol efflux.

RUT reduced atherosclerotic lesions in ApoE$^{-/-}$ mice

The above-mentioned in vitro discovery was then translated into an in vivo test. Eight-week-old female ApoE$^{-/-}$ mice were fed with a chow diet or HFD for 2 months, with or without RUT treatment. ApoE$^{-/-}$ mice displayed a slow progression of atherosclerosis when fed a normal chow diet; however, ORO-positive en face atherosclerotic lesions were found in the aortic arches and thoracic aortas in ApoE$^{-/-}$ mice on HFD, especially in the brachiocephalic trunk arteries (**Fig. 4A-b**). In contrast, ApoE$^{-/-}$ mice treated with RUT showed fewer en face lesions along the aorta as compared with the untreated model group (Fig. 4A-c–e). With respect to the untreated model groups, the reduction of en face lesions was 68.43 ± 10.52, 70.23 ± 12.69, and 85.56 ± 14.53% in RUT (L), RUT (M), or RUT (H) groups, respectively ($P < 0.01$) (Fig. 4B). Quantitative analysis of atherosclerosis was also performed by measuring the extent of the ORO staining for the cryosections taken from the aortic sinuses. ORO-stained sections were from the complete aortic valve cusp attached to the aorta. The plaque area in the aortic sinus was significantly reduced in ApoE$^{-/-}$ mice treated with RUT as compared with ApoE$^{-/-}$ mice in the untreated model group (Fig. 4C). While the mean area of the untreated model group was 114.60 ± 15.84 × 10^4 (μm^2 ± SD), the mean area of the RUT-treated groups was 87.07 ± 8.89 × 10^4, 65.85 ± 3.81 × 10^4, and 47.40 ± 15.14 × 10^4 (μm^2 ± SD) for the RUT (L), RUT (M), and RUT (H) groups, respectively ($P < 0.01$; Fig. 4D). The control group had a mean area value of 24.99 ± 10.72 × 10^4 (μm^2 ± SD) in this experiment (Fig. 4D).

The ORO-positive lipid area in liver tissue of the ApoE$^{-/-}$ mice treated with RUT significantly reduced as compared with the model group (Fig. 4E). Mac-3 was a macrophage-specific antibody to identify foam cells derived from macrophages. Mac-3-positive macrophages were detected in abundance in lesions of the aortic walls in ApoE$^{-/-}$ mice on an HFD (Fig. 4E). In contrast, ApoE$^{-/-}$ mice treated with RUT showed significantly less Mac-3 staining as compared with the untreated model group (Fig. 4E). Filipin staining is selective for cholesterol and thus was used in this study as well. The results indicated that the lipid components in the lesions of the model group were mainly composed of cholesterol (Fig. 4E). There were a few Mac-3 and filipin staining areas observed in the aortic sinuses of the ApoE$^{-/-}$ mice on a chow diet (Fig. 4E). In addition, there were no significant differences in H&E staining (Fig. 4E) and plasma levels of aspartate aminotransferase (AST) and alanine transaminase (ALT) (supplementary Table II) in ApoE$^{-/-}$ mice treated with or without RUT, which indicated that ApoE$^{-/-}$ mice treated with RUT did not show significant toxicity in hepatocytes.

RUT lowers plasma TC and TG

To investigate the effect of RUT on lipid homeostasis in detail, plasma lipid levels of ApoE$^{-/-}$ mice treated with or without RUT were determined (**Table 2**). The ApoE$^{-/-}$ mice fed on HFD for 8 weeks showed elevated plasma level of TC, HDL-C, LDL-C, and TG, in comparison with the ApoE$^{-/-}$ mice fed a normal chow diet (764 ± 48 vs. 351 ± 29; 93 ± 16 vs. 36 ± 10; 454 ± 37 vs. 172 ± 48; 110 ± 15 vs. 69 ± 14 mg/dl, $P < 0.01$). After 8-week RUT therapy, plasma TC in the ApoE$^{-/-}$ mice was 652 ± 50, 601 ± 19, and 525 ± 37 ($P < 0.01$) mg/dl for the RUT (L), RUT (M), and RUT (H) groups, respectively, significantly lower than that of the untreated model group (688 ± 30 mg/dl); LDL-C level in RUT (L), RUT (M), and RUT (H) groups also decreased significantly as compared with the untreated model group [390 ± 46, 382 ± 46, or 378 ± 28 vs. 454 ± 37 mg/dl ($P < 0.01$), respectively]; TG level in RUT (L), RUT (M), and RUT (H) groups decreased significantly as compared with the untreated model group [79 ± 14, 81.15 ± 10.44 or 75 ± 11 vs. 110 ± 15 mg/dl ($P<0.01$), respectively];

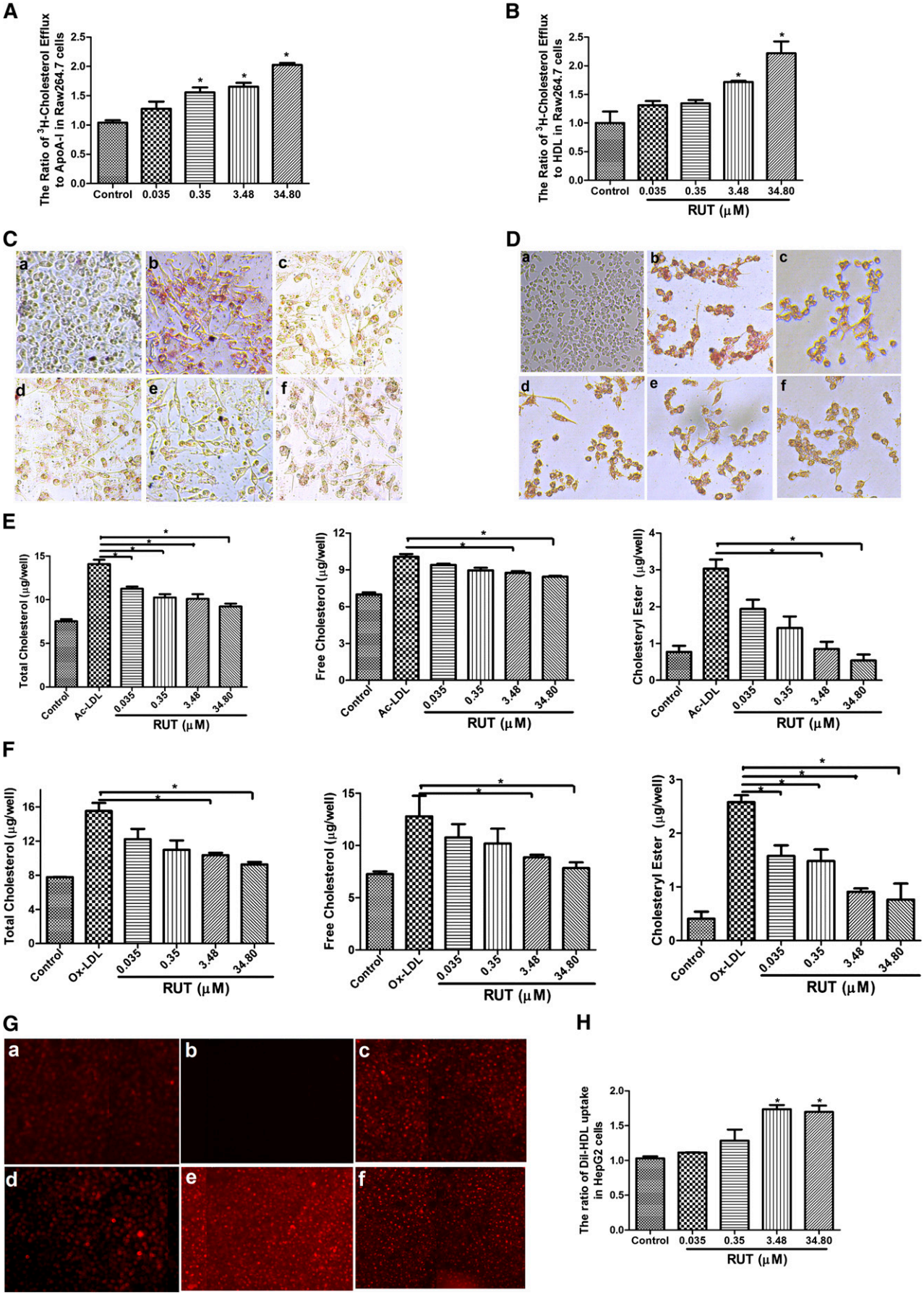
A
The Ratio of ^{3}H-Cholesterol Efflux to ApoA-I in Raw264.7 cells
Control
0.035
0.35
3.48
34.80
B
The Ratio of ^{3}H-Cholesterol Efflux to HDL in Raw264.7 cells
RUT (μM)
C
D
E
Total Cholesterol (μg/well)
Free Cholesterol (μg/well)
Cholesteryl Ester (μg/well)
Ac-LDL
RUT (μM)
F
Ox-LDL
G
H
The ratio of Dil-HDL uptake in HepG2 cells

and plasma HDL-C increased slightly in RUT treated groups as compared with the untreated model group. Significant differences in food intake and water consumed were not observed between ApoE$^{-/-}$ mice treated with or without RUT.

RUT increased fecal cholesterol in ApoE$^{-/-}$ mice

After 8-week RUT therapy, cholesterol in liver, small intestine, and feces of ApoE$^{-/-}$ mice treated with or without RUT was measured as described in Methods. Specifically, liver cholesterol in the RUT (M) and RUT (H) groups decreased significantly as compared with the untreated model group [52.61 ± 1.92 or 29.95 ± 5.51 vs. 80.08 ± 4.31 μmol/g protein ($P < 0.05$), respectively] (**Fig. 5A**); intestine cholesterol in the RUT (M) and RUT (H) groups was 24.0 ± 1.08 and 23.05 ± 3.00 μmol/g protein, respectively, significantly lower than that of the model group (35.23 ± 1.53 μmol/g protein) ($P < 0.05$) (Fig. 5B).

Because plasma, liver, and intestine cholesterol levels decreased to a significant extent, we investigated whether this translated to increased fecal excretion. Feces were collected in the last 24 h, just before mice were euthanized. Indeed, we found that cholesterol excretion was strongly increased in RUT-treated mice. Cholesterol in the feces of the RUT (L), RUT (M), and RUT (H) groups was 168.46 ± 7.67, 177.87 ± 1.74, and 220.64 ± 4.00 μmol/g protein, respectively, significantly higher than that of the untreated model group (108.61 ± 14.77 μmol/g protein) ($P < 0.05$). In all, our data demonstrated that RUT might enhance RCT (Fig. 5C).

RUT induced ABCA1 and SR-BI expression in liver of ApoE$^{-/-}$ mice

Considering our previous observation, the expression levels of the various genes involved in the RCT process in liver from control and RUT-treated mice were measured. The expression of ABCA1 and SR-BI, which are the key receptors of RCT, was significantly increased by RUT treatment at both mRNA and protein levels (Fig. 5D, E). As shown in Fig. 5D, E, RUT slightly increased ABCG1 expression but did not alter CD36 and SREBP-1c expression. In addition, Western blot analysis showed that RUT increased FAS expression in RUT (M) and RUT (H) (Fig. 5E). These results are in agreement with those obtained in vitro (Fig. 1F, G).

In all, the results showed that the antiatherosclerotic effect of RUT should be through promoting RCT by upregulating ABCA1 and SR-BI/CLA-1 expression in ApoE$^{-/-}$ mice.

RUT promoted macrophage-to-feces RCT in vivo

RCT is a pathway network through which the accumulated cholesterol could be transported from vessel wall to liver for excretion. To investigate whether RUT promotes RCT, radio-labeled macrophages were injected in C57/BL6 or ApoE$^{-/-}$ mice treated with CMC-Na or 20 mg/kg RUT. As shown in **Fig. 6**, ^{3}H-tracer recovery in plasma and liver was higher in C57/BL6 (Fig. 6A, B) and ApoE$^{-/-}$ mice (Fig. 6D, E) treated with the RUT at 48 h after injection than the CMC-Na group, but the difference was not statistically significant. The ^{3}H-tracer recovery was also measured in feces after chemical extraction (Fig. 6C, F). However, there were significant 185% ($P = 0.06$), 148% ($P = 0.06$), and 174% ($P = 0.08$) increases in the ^{3}H-total sterol, cholesterol, and bile acid fecal excretion for C57/BL6 mice treated with RUT (Fig. 6C). There were also significant 245% ($P < 0.05$), 162% ($P < 0.05$), and 412% ($P < 0.05$) increases in the ^{3}H-total sterol, cholesterol, and bile acid fecal excretion for ApoE$^{-/-}$ mice treated with RUT (Fig. 6F). Overall, these data demonstrated that administration of RUT to mice preinjected with ^{3}H-cholesterol-labeled macrophages markedly increased fecal ^{3}H-tracer excretion, thus providing direct evidence that RUT promoted macrophage-to-feces RCT in vivo.

DISCUSSION

RCT is a pathway through which the accumulated cholesterol could be transported from vessel wall to liver for excretion in the bile and ultimately the feces. ABCA1 and SR-BI/CLA-1 are key receptors in RCT. The present study was designed to find novel antiatherosclerotic agents by upregulating expression of ABCA1 and SR-BI/CLA-1 from natural or synthetic compounds.

RUT was discovered to be a positive candidate. RUT is a quinazolinocarboline alkaloid identified from *Evodia*

Fig. 3. Effects of RUT on cholesterol efflux and HDL uptake in vitro. A, B: RUT stimulated cholesterol efflux from RAW264.7 (A) to ApoA-I or HDL (B). Data are the means ± SD of three independent experiments and expressed as a relative value to control (* $P < 0.05$ vs. control). C–F: RAW264.7 macrophages were coincubated with RUT (0.035, 0.35, 3.48, and 34.80 μM) and Ac-LDL or Ox-LDL (80 μg/ml) for 24 h. After incubation, cells were fixed and stained with ORO (C, D), or intracellular cholesterol was extracted and determined by the Cholesterol Assay Kit (E, F). The study samples were negative control (a), Ac-LDL/Ox-LDL (control) (b), both Ac-LDL/Ox-LDL and 0.035 μM RUT (c), both Ac-LDL/Ox-LDL and 0.35 μM RUT (d), both Ac-LDL/Ox-LDL and 3.48 μM RUT (e), and both Ac-LDL/Ox-LDL and 34.80 μM RUT (f). The magnification of each panel is ×100. * $P < 0.05$ versus Ac-LDL/Ox-LDL-treated alone group. Cholesterol content was measured as μg per 10^{6} cells every 6 wells. The results were from three independent experiments. Data are means ± SEM [* $P < 0.05$ vs. control group (Ac-LDL/Ox-LDL only)]. G, H: RUT suppresses the uptake of DiI-HDL by HepG2 cells. HepG2 cells were incubated with RUT (0.035, 0.35, 3.48, and 34.80 μM) or vehicle (0.1% DMSO) for 24 h as described in Methods. The study samples were as follows: DiI-HDL (control) (a), negative control (b), both DiI-HDL and 0.035 μM RUT (c), both DiI-HDL and 0.35 μM RUT (d), both DiI-HDL and 3.48 μM RUT (e), and both DiI-HDL and 34.80 μM RUT (f). DiI-HDL uptake was assessed by confocal microscopy (G) and determined by a microplate reader (H) expressed as fold of the control. The results were from three independent experiments. Data are means ± SEM [* $P < 0.05$ vs. control group (DiI-HDL only)].

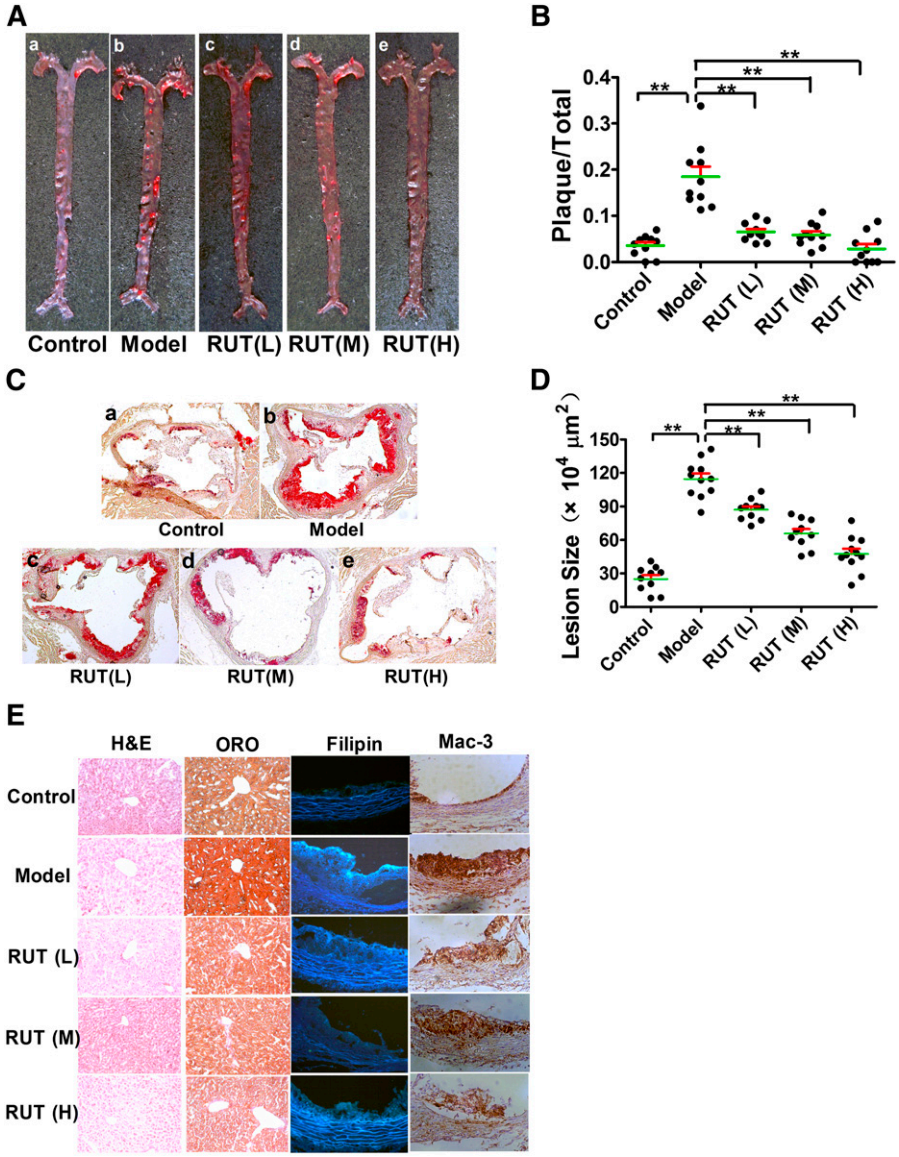

Fig. 4. RUT reduced atherosclerotic lesions in ApoE$^{-/-}$ mice. ApoE$^{-/-}$ mice were treated as described in Methods. Representative images of en face (A) and aortic sinus section (C) staining for the lesions of each group of mice were shown. Quantitative analysis of en face (B) and aortic sinus section (100×) (D) staining lesions for 2-month-old ApoE$^{-/-}$ mice was shown to demonstrate the inhibitory effect of RUT on atherosclerosis. Values are expressed as means ± SEM, n = 10–12. * $P < 0.05$; ** $P < 0.01$. E: Histology and immunohistochemical examination of liver with H&E (200×) or ORO (200×) staining, and aortic sinus by filipin (200×) or Mac-3 (200×).

rutaecapa. The plant is an herb in China used for gastrointestinal disorders, cardiovascular diseases, headache, amenorrhea, abdominal pain, dysentery, and postpartum hemorrhage in traditional Chinese medicine (42, 43). In this manuscript, we identified for the first time that RUT had antiatherogenic effects in vitro and in vivo through upregulating ABCA1 and SR-BI/CLA-1 expression within RCT.

RUT not only promoted cholesterol efflux in vitro (Fig. 3), but also suppressed blood cholesterol (Table 2) in the ApoE$^{-/-}$ mice treated with RUT. Accompanied with the cholesterol-lowering effect (Table 2), reduced atherosclerotic lesions were evidenced not only in en face arteries, but also in aortic sinuses after 8-week RUT treatment (Fig. 4). We also observed a reduced macrophage activity and decreased cholesterol content in the aortic sinus plaques of ApoE$^{-/-}$ mice treated with RUT (Fig. 4). Besides therapeutic efficacy, the animal studies ensured safety of RUT in vivo. The LD_{50} of RUT intragastrically in ICR mice was >2,000 mg/kg, ~50 times higher than the treatment doses (supplementary Table I). H&E staining of livers, kidneys, and hearts showed that cell survival was not interrupted by RUT (supplementary Fig. I).

RUT decreased liver and intestine cholesterol and increased fecal cholesterol output in ApoE$^{-/-}$ mice (Fig. 5A–C), which indicated that RUT might promote RCT in

TABLE 2. Plasma lipids in a ApoE$^{-/-}$ mice fed a normal chow diet or HFD (mg/dl)

Group	n	TC (mg/dl)	HDL (mg/dl)	LDL (mg/dl)	TG (mg/dl)
Control	12	351 ± 29	36 ± 10	172 ± 48	69 ± 14
Model	12	764 ± 48[a]	93 ± 16[a]	454 ± 37[a]	110 ± 15[a]
RUT (L)	12	652 ± 50[b]	95 ± 19	390 ± 46[c]	79 ± 14[b]
RUT (M)	12	601 ± 19[b]	92 ± 26	382 ± 46[c]	81 ± 10[b]
RUT (H)	12	525 ± 37[b]	97 ± 24	378 ± 28[c]	75 ± 11[b]
Simvastatin	12	566 ± 53[b]	97 ± 16	372 ± 28[b]	77 ± 12[b]

ApoE$^{-/-}$ mice were fed on a normal chow or HFD for 8 weeks. Values are expressed as means ± SD. The number of animals in each group is indicated by n.

[a]$P < 0.01$, mice on a HFD (model group) compared with that with a chow diet (control group).

[b]$P < 0.01$, RUT treatment versus no treatment (model group).

[c]$P < 0.05$, RUT treatment versus no treatment (model group).

vivo. Fig. 6 showed that RUT caused a small elevation in the amount of labeled cholesterol in transitory RCT cholesterol pools, plasma, and liver but had greater effects on accumulation of labeled cholesterol in the cumulative end pool, feces. Therefore, our data suggested that RUT was effective in delivering cholesterol to the liver pool destined for excretion and conversion to bile acids.

ABCA1 and SR-BI/CLA-1 are the most important transporter and receptor within RCT. RUT could upregulate expression of ABCA1 and SR-BI/CLA-1. Increasing ABCA1 expression could facilitate cholesterol efflux in macrophages. Increasing SR-BI/CLA-1 expression could facilitate HDL-mediated cholesterol efflux from the arterial wall and hepatic uptake of HDL-C. HDL may prevent atherosclerotic development by engaging in RCT from the arterial wall to the liver and blocking Ox-LDL accumulated in the artery (44). Lowering TC and LDL-C might contribute, at least in part, to the beneficial effect of RUT in plaque regression. Additionally, RUT also increased ABCG1 expression, which also facilitated RCT. Interestingly, RUT does not alter CD36 expression level; therefore, it should not increase cholesterol uptake in foam cells. Thus, we speculate that the increased cholesterol efflux and inhibited lipid accumulation in vitro and in vivo by RUT reflected a synergy of multiple-target effects in the RCT system.

RUT was demonstrated to exhibit an antiatherogenic effect by upregulating ABCA1 and SR-BI/CLA-1 expression.

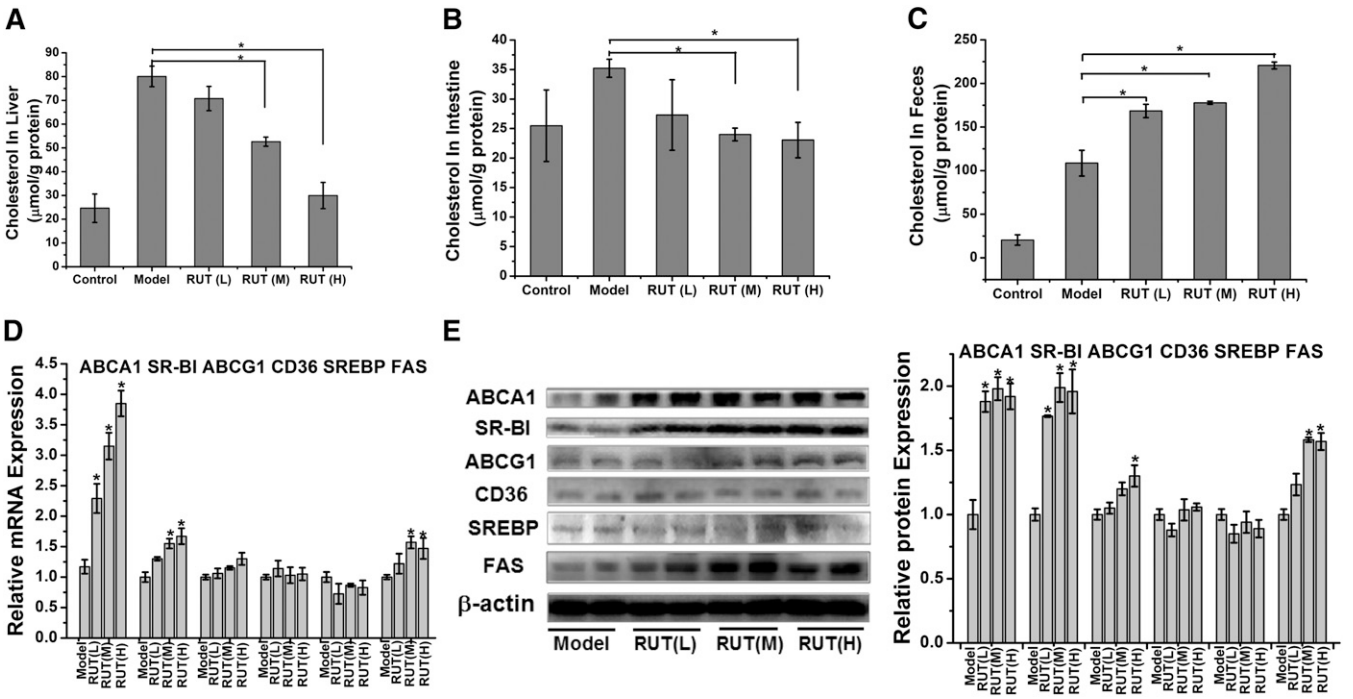

Fig. 5. Effects of RUT on cholesterol distribution in tissue and related gene expression in liver of ApoE$^{-/-}$ mice. Effects of RUT on cholesterol distribution in liver (A), intestine (B), and feces (C) in ApoE$^{-/-}$ mice. ApoE$^{-/-}$ mice were treated as described in Methods. RUT treatment lowers liver (A) and intestine cholesterol (B) and increases fecal cholesterol (C) in ApoE$^{-/-}$ mice on HFD. The content of cholesterol was determined as described in Methods. Data are expressed as means ± SEM; n = 12. Effects of RUT on gene expression were measured by RT-PCR (D) and Western blotting (E) analysis in liver in ApoE$^{-/-}$ mice. For RT-PCR, data are expressed as means ± SEM (* $P <$ 0.05 vs. model group). n = 12 mice per group. For Western blot, representative immunoblot results are shown (E), and the abundances were normalized to that of β-actin (means ± SEM, * $P < 0.05$ vs. model group).

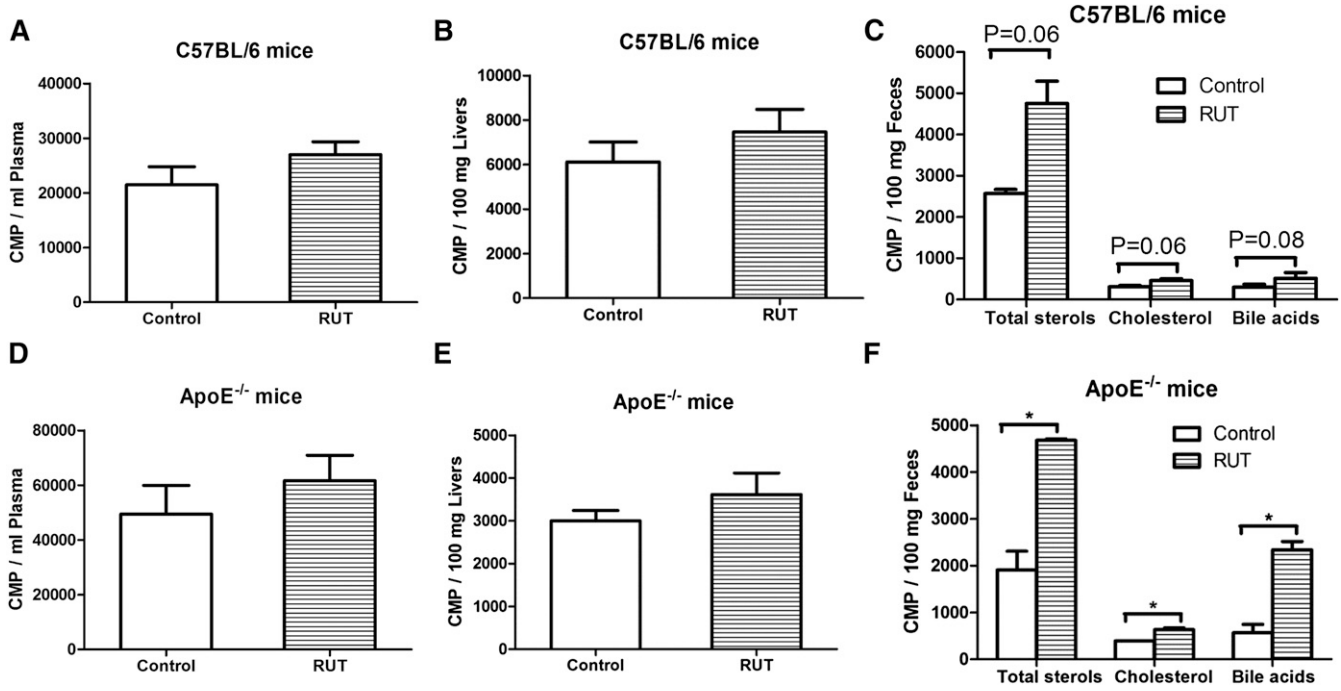

Fig. 6. Effects of RUT on RCT in vivo. Plasma, liver, and fecal ^{3}H-tracer distributions in male wild-type mice (A–C) and ApoE$^{-/-}$ mice (D–F). C57BL/6 mice on chow diet were pretreated with either CMC-Na or RUT for 14 days. ApoE$^{-/-}$ mice on HFD were pretreated with either CMC-Na or RUT for 8 weeks. Then ^{3}H-cholesterol-labeled J774 cells were injected intraperitoneally. Forty-eight hours later, mice were euthanized. Plasma, liver, fecal, and bile ^{3}H tracer were counted in a liquid scintillation counter as described in Methods. Values are expressed as means ± SEM. * $P < 0.05$ versus CMC-Na-treated group. n = 6 mice per group.

SiRNA assays showed that the upregulating effect of RUT on ABCA1 and SR-BI/CLA-1 expression was related to LXRα and LXRβ activation (Fig. 2C, D). A common theme in transcriptional regulation by NRs is the involvement of a highly related protein family (45). The SRC protein family comprises important coactivators of NRs. SRC-1 forms complexes with the cointegrator CBP, whose histone acetyltransferase activity is not only required for histone modifications but may also regulate coactivator-NR interactions (46). RUT recruited coactivator peptides SRC1-2, SRC1-4, SRC2-2, and CBP-1 to LXRα and LXRβ LBDs (Fig. 2E, F). Therefore, we conclude that RUT recruited coactivator peptides SRC1-2, SRC1-4, and SRC2-2 and cointegrator CBP-1 to form complexes to interact with LXRα or LXRβ LBD and then upregulated ABCA1 and SR-BI/CLA-1 expression.

Some studies have explained partial mechanisms of the cardiovascular protective activity of RUT, including stimulating the calcitonin gene-related peptide release (47) anti-inflammatory activities (48–50). In this manuscript, we also found that RUT could inhibit some inflammatory factors including TNF-α, monocyte chemoattractant protein-1, and interleukin-8 expression (supplementary Fig. III) in ApoE$^{-/-}$ mice, which might contribute to the good antiatherosclerotic effect. Our present study for the first time gives experimental evidence that RUT can effectively reduce atherosclerosis through upregulating ABCA1 and SR-BI/CLA-1 within RCT. Moreover, we think that the most important antiatherosclerotic mechanism of RUT is through promoting RCT in vivo.

In summary, our present study for the first time demonstrates that RUT can effectively reduce atherosclerosis through upregulating ABCA1 and SR-BI within RCT. Our study suggests that RUT might be promising in the treatment of atherosclerosis, and ABCA1 and SR-BI/CLA-1 could be used as effective therapeutic targets for drug discovery against atherosclerosis.

We thank Wei Huang, Juan Wang, and Qiang Shen from the Institute of Cardiovascular Sciences and Key Laboratory of Molecular Cardiovascular Sciences of Peking University for their expert technical assistance during the course of animal studies.

REFERENCES

1. Pennings, M., I. Meurs, D. Ye, R. Out, M. Hoekstra, T. J. Van Berkel, and M. Van Eck. 2006. Regulation of cholesterol homeostasis in macrophages and consequences for atherosclerotic lesion development. *FEBS Lett.* **580:** 5588–5596.
2. Francone, O. L. 2003. SR-BI: a new player in an old game. *Arterioscler. Thromb. Vasc. Biol.* **23:** 1486–1487.
3. Ohashi, R., H. Mu, X. Wang, Q. Yao, and C. Chen. 2005. Reverse cholesterol transport and cholesterol efflux in atherosclerosis. *QJM.* **98:** 845–856.
4. Cuchel, M., and D. J. Rader. 2006. Macrophage reverse cholesterol transport: key to the regression of atherosclerosis? *Circulation.* **113:** 2548–2555.
5. Fougerat, A., S. Gayral, P. Gourdy, A. Schambourg, T. Ruckle, M. K. Schwarz, C. Rommel, E. Hirsch, J. F. Arnal, J. P. Salles, et al. 2008. Genetic and pharmacological targeting of phosphoinositide 3-kinase-gamma reduces atherosclerosis and favors plaque stability by modulating inflammatory processes. *Circulation.* **117:** 1310–1317.
6. Yvan-Charvet, L., N. Wang, and A. R. Tall. 2010. Role of HDL, ABCA1, and ABCG1 transporters in cholesterol efflux and immune responses. *Arterioscler. Thromb. Vasc. Biol.* **30:** 139–143.

7. Tall, A. R. 2008. Cholesterol efflux pathways and other potential mechanisms involved in the athero-protective effect of high density lipoproteins. *J. Intern. Med.* **263:** 256–273.
8. Yancey, P. G., A. E. Bortnick, G. Kellner-Weibel, M. de la Llera-Moya, M. C. Phillips, and G. H. Rothblat. 2003. Importance of different pathways of cellular cholesterol efflux. *Arterioscler. Thromb. Vasc. Biol.* **23:** 712–719.
9. Zarubica, A., D. Trompier, and G. Chimini. 2007. ABCA1, from pathology to membrane function. *Pflugers Arch.* **453:** 569–579.
10. Joyce, C., L. Freeman, H. B. Brewer, Jr., and S. Santamarina-Fojo. 2003. Study of ABCA1 function in transgenic mice. *Arterioscler. Thromb. Vasc. Biol.* **23:** 965–971.
11. Yvan-Charvet, L., C. Welch, T. A. Pagler, M. Ranalletta, M. Lamkanfi, S. Han, M. Ishibashi, R. Li, N. Wang, and A. R. Tall. 2008. Increased inflammatory gene expression in ABC transporter-deficient macrophages: free cholesterol accumulation, increased signaling via toll-like receptors, and neutrophil infiltration of atherosclerotic lesions. *Circulation.* **118:** 1837–1847.
12. Price, M. J., and P. K. Shah. 2002. New strategies in managing and preventing atherosclerosis: focus on HDL. *Rev. Cardiovasc. Med.* **3:** 129–137.
13. Joyce, C. W., M. J. Amar, G. Lambert, B. L. Vaisman, B. Paigen, J. Najib-Fruchart, R. F. Hoyt, Jr., E. D. Neufeld, A. T. Remaley, D. S. Fredrickson, et al. 2002. The ATP binding cassette transporter A1 (ABCA1) modulates the development of aortic atherosclerosis in C57BL/6 and apoE-knockout mice. *Proc. Natl. Acad. Sci. USA.* **99:** 407–412.
14. Joyce, C. W., E. M. Wagner, F. Basso, M. J. Amar, L. A. Freeman, R. D. Shamburek, C. L. Knapper, J. Syed, J. Wu, B. L. Vaisman, et al. 2006. ABCA1 overexpression in the liver of LDLr-KO mice leads to accumulation of pro-atherogenic lipoproteins and enhanced atherosclerosis. *J. Biol. Chem.* **281:** 33053–33065.
15. Calvo, D., and M. A. Vega. 1993. Identification, primary structure, and distribution of CLA-1, a novel member of the CD36/LIMPII gene family. *J. Biol. Chem.* **268:** 18929–18935.
16. Rothblat, G. H., M. de la Llera-Moya, V. Atger, G. Kellner-Weibel, D. L. Williams, and M. C. Phillips. 1999. Cell cholesterol efflux: integration of old and new observations provides new insights. *J. Lipid Res.* **40:** 781–796.
17. Acton, S. L., K. F. Kozarsky, and A. Rigotti. 1999. The HDL receptor SR-BI: a new therapeutic target for atherosclerosis? *Mol. Med. Today.* **5:** 518–524.
18. Ji, Y., B. Jian, N. Wang, Y. Sun, M. L. Moya, M. C. Phillips, G. H. Rothblat, J. B. Swaney, and A. R. Tall. 1997. Scavenger receptor BI promotes high density lipoprotein-mediated cellular cholesterol efflux. *J. Biol. Chem.* **272:** 20982–20985.
19. Rigotti, A., H. E. Miettinen, and M. Krieger. 2003. The role of the high-density lipoprotein receptor SR-BI in the lipid metabolism of endocrine and other tissues. *Endocr. Rev.* **24:** 357–387.
20. Gao, J., Y. Xu, Y. Yang, Y. Yang, Z. Zheng, W. Jiang, B. Hong, X. Yan, and S. Si. 2008. Identification of upregulators of human ATP-binding cassette transporter A1 via high-throughput screening of a synthetic and natural compound library. *J. Biomol. Screen.* **13:** 648–656.
21. Yang, Y., Z. Zhang, W. Jiang, L. Gao, G. Zhao, Z. Zheng, M. Wang, S. Si, and B. Hong. 2007. Identification of novel human high-density lipoprotein receptor up-regulators using a cell-based high-throughput screening assay. *J. Biomol. Screen.* **12:** 211–219.
22. Xu, Y., J. Wang, Y. Bao, W. Jiang, L. Zuo, D. Song, B. Hong, and S. Si. 2010. Identification of two antagonists of the scavenger receptor CD36 using a high-throughput screening model. *Anal. Biochem.* **400:** 207–212.
23. Okamoto, Y., S. Kihara, N. Ouchi, M. Nishida, Y. Arita, M. Kumada, K. Ohashi, N. Sakai, I. Shimomura, H. Kobayashi, et al. 2002. Adiponectin reduces atherosclerosis in apolipoprotein E-deficient mice. *Circulation.* **106:** 2767–2770.
24. Zhang, X., R. Qi, X. Xian, F. Yang, M. Blackstein, X. Deng, J. Fan, C. Ross, J. Karasinska, M. R. Hayden, et al. 2008. Spontaneous atherosclerosis in aged lipoprotein lipase-deficient mice with severe hypertriglyceridemia on a normal chow diet. *Circ. Res.* **102:** 250–256.
25. Bietrix, F., E. Lombardo, C. P. van Roomen, R. Ottenhoff, M. Vos, P. C. Rensen, A. J. Verhoeven, J. M. Aerts, and A. K. Groen. 2010. Inhibition of glycosphingolipid synthesis induces a profound reduction of plasma cholesterol and inhibits atherosclerosis development in APOE*3 Leiden and low-density lipoprotein receptor−/− mice. *Arterioscler. Thromb. Vasc. Biol.* **30:** 931–937.
26. Bijl, N., C. P. van Roomen, V. Triantis, M. Sokolovic, R. Ottenhoff, S. Scheij, M. van Eijk, R. G. Boot, J. M. Aerts, and A. K. Groen. 2009. Reduction of glycosphingolipid biosynthesis stimulates biliary lipid secretion in mice. *Hepatology.* **49:** 637–645.
27. Jeon, H. J., J. H. Choi, I. H. Jung, J. G. Park, M. R. Lee, M. N. Lee, B. Kim, J. Y. Yoo, S. J. Jeong, D. Y. Kim, et al. 2010. CD137 (4–1BB) deficiency reduces atherosclerosis in hyperlipidemic mice. *Circulation.* **121:** 1124–1133.
28. Leger, A. J., L. M. Mosquea, L. Li, W. Chuang, J. Pacheco, K. Taylor, Z. Luo, P. Piepenhagen, R. Ziegler, R. Moreland, et al. 2011. Adeno-associated virus-mediated expression of acid sphingomyelinase decreases atherosclerotic lesion formation in apolipoprotein E(−/−) mice. *J. Gene Med.* **13:** 324–332.
29. Norata, G. D., P. Marchesi, V. K. Pulakazhi Venu, F. Pasqualini, A. Anselmo, F. Moalli, I. Pizzitola, C. Garlanda, A. Mantovani, and A. L. Catapano. 2009. Deficiency of the long pentraxin PTX3 promotes vascular inflammation and atherosclerosis. *Circulation.* **120:** 699–708.
30. Zhang, Y., I. Zanotti, M. P. Reilly, J. M. Glick, G. H. Rothblat, and D. J. Rader. 2003. Overexpression of apolipoprotein A-I promotes reverse transport of cholesterol from macrophages to feces in vivo. *Circulation.* **108:** 661–663.
31. Naik, S. U., X. Wang, J. S. Da Silva, M. Jaye, C. H. Macphee, M. P. Reilly, J. T. Billheimer, G. H. Rothblat, and D. J. Rader. 2006. Pharmacological activation of liver X receptors promotes reverse cholesterol transport in vivo. *Circulation.* **113:** 90–97.
32. Terao, Y., M. Ayaori, M. Ogura, E. Yakushiji, H. Uto-Kondo, T. Hisada, H. Ozasa, S. Takiguchi, K. Nakaya, M. Sasaki, et al. 2011. Effect of sulfonylurea agents on reverse cholesterol transport in vitro and vivo. *J. Atheroscler. Thromb.* **18:** 513–530.
33. Tanigawa, H., J. T. Billheimer, J. Tohyama, Y. Zhang, G. Rothblat, and D. J. Rader. 2007. Expression of cholesteryl ester transfer protein in mice promotes macrophage reverse cholesterol transport. *Circulation.* **116:** 1267–1273.
34. Tancevski, I., E. Demetz, P. Eller, K. Duwensee, J. Hoefer, C. Heim, U. Stanzl, A. Wehinger, K. Auer, R. Karer, et al. 2010. The liver-selective thyromimetic T-0681 influences reverse cholesterol transport and atherosclerosis development in mice. *PLoS ONE.* **5:** e8722.
35. Zheng, Z., Y. Yang, H. Shao, Z. Liu, X. Lu, Y. Xu, X. He, W. Jiang, Q. Jiang, B. Zhao, et al. 2011. Two thiophenes compounds are partial peroxisome proliferator-activated receptor alpha/gamma dual agonists. *Biol. Pharm. Bull.* **34:** 1631–1634.
36. Smith, J. D., W. Le Goff, M. Settle, G. Brubaker, C. Waelde, A. Horwitz, and M. N. Oda. 2004. ABCA1 mediates concurrent cholesterol and phospholipid efflux to apolipoprotein A-I. *J. Lipid Res.* **45:** 635–644.
37. Xu, Y., Y. Xu, Y. Bao, B. Hong, and S. Si. 2011. Identification of dehydroxytrichostatin A as a novel up-regulator of the ATP-binding cassette transporter A1 (ABCA1). *Molecules.* **16:** 7183–7198.
38. Liu, Z., J. Wang, E. Huang, S. Gao, H. Li, J. Lu, K. Tian, P. J. Little, X. Shen, S. Xu, et al. 2014. Tanshinone IIA suppresses cholesterol accumulation in human macrophages: role of heme oxygenase-1. *J. Lipid Res.* **55:** 201–213.
39. Marleau, S., D. Harb, K. Bujold, R. Avallone, K. Iken, Y. Wang, A. Demers, M. G. Sirois, M. Febbraio, R. L. Silverstein, et al. 2005. EP 80317, a ligand of the CD36 scavenger receptor, protects apolipoprotein E-deficient mice from developing atherosclerotic lesions. *FASEB J.* **19:** 1869–1871.
40. Lu, K. Y., L. C. Ching, K. H. Su, Y. B. Yu, Y. R. Kou, S. H. Hsiao, Y. C. Huang, C. Y. Chen, L. C. Cheng, C. C. Pan, et al. 2010. Erythropoietin suppresses the formation of macrophage foam cells: role of liver X receptor alpha. *Circulation.* **121:** 1828–1837.
41. George, J., A. Afek, P. Keren, I. Herz, I. Goldberg, R. Haklai, Y. Kloog, and G. Keren. 2002. Functional inhibition of Ras by S-trans,trans-farnesyl thiosalicylic acid attenuates atherosclerosis in apolipoprotein E knockout mice. *Circulation.* **105:** 2416–2422.
42. Lee, S. H., J. K. Son, B. S. Jeong, T. C. Jeong, H. W. Chang, E. S. Lee, and Y. Jahng. 2008. Progress in the studies on rutaecarpine. *Molecules.* **13:** 272–300.
43. Jia, S., and C. Hu. 2010. Pharmacological effects of rutaecarpine as a cardiovascular protective agent. *Molecules.* **15:** 1873–1881.
44. Choi, B. G., G. Vilahur, J. F. Viles-Gonzalez, and J. J. Badimon. 2006. The role of high-density lipoprotein cholesterol in atherothrombosis. *Mt. Sinai J. Med.* **73:** 690–701.
45. Choi, K. C., S. Y. Oh, H. B. Kang, Y. H. Lee, S. Haam, H. I. Kim, K. Kim, Y. H. Ahn, K. S. Kim, and H. G. Yoon. 2008. The functional relationship between co-repressor N-CoR and SMRT in mediating transcriptional repression by thyroid hormone receptor alpha. *Biochem. J.* **411:** 19–26.

46. Rachez, C., M. Gamble, C. P. Chang, G. B. Atkins, M. A. Lazar, and L. P. Freedman. 2000. The DRIP complex and SRC-1/p160 coactivators share similar nuclear receptor binding determinants but constitute functionally distinct complexes. *Mol. Cell. Biol.* **20:** 2718–2726.
47. Peng, J., and Y. J. Li. 2010. The vanilloid receptor TRPV1: role in cardiovascular and gastrointestinal protection. *Eur. J. Pharmacol.* **627:** 1–7.
48. Moon, T. C., M. Murakami, I. Kudo, K. H. Son, H. P. Kim, S. S. Kang, and H. W. Chang. 1999. A new class of COX-2 inhibitor, rutaecarpine from Evodia rutaecarpa. *Inflamm. Res.* **48:** 621–625.
49. Ko, H. C., Y. H. Wang, K. T. Liou, C. M. Chen, C. H. Chen, W. Y. Wang, S. Chang, Y. C. Hou, K. T. Chen, C. F. Chen, et al. 2007. Anti-inflammatory effects and mechanisms of the ethanol extract of Evodia rutaecarpa and its bioactive components on neutrophils and microglial cells. *Eur. J. Pharmacol.* **555:** 211–217.
50. Heo, S. K., H. J. Yun, H. S. Yi, E. K. Noh, and S. D. Park. 2009. Evodiamine and rutaecarpine inhibit migration by LIGHT via suppression of NADPH oxidase activation. *J. Cell. Biochem.* **107:** 123–133.